



Effects of swift heavy ion irradiation on the performance of HfO₂-based resistive random access memory devices

N. Arun¹, L. D. Varma Sangani², K. Vinod Kumar³, A. Mangababu³, M. Ghanashyam Krishna^{1,3}, A. P. Pathak³, and S. V. S. Nageswara Rao^{1,3,*}

¹Centre for Advanced Studies in Electronics Science and Technology (CASEST), School of Physics, University of Hyderabad, Hyderabad 500 046, India

²Department of Condensed Matter Physics and Materials Science, Tata Institute of Fundamental Research, Homi Bhabha Road, Mumbai 400005, India

³School of Physics, University of Hyderabad, Hyderabad 500 046, India

Received: 26 September 2020

Accepted: 3 December 2020

Published online:

6 January 2021

© The Author(s), under exclusive licence to Springer Science+Business Media, LLC part of Springer Nature 2021

ABSTRACT

In this work, the effects of 120 MeV Ag ion irradiation on the switching properties of Au/HfO₂/Au-based Resistive Random Access Memory (RRAM) devices are reported. The ion fluence is varied between 5×10^{10} and 5×10^{12} ions/cm² while two device sizes, with active areas $10 \mu\text{m} \times 10 \mu\text{m}$ and $20 \mu\text{m} \times 20 \mu\text{m}$, are tested. In each case, 16 devices are subjected to ion irradiation and it is shown that the set voltages are generally lower and the spread in the switching voltages is reduced for the irradiated samples in comparison to the pristine devices. The existence of a critical dose of 5×10^{11} ions/cm² up to which an improvement in the device performance is observed. Photoluminescence studies indicate the presence of oxygen-related vacancies in both pristine and irradiated samples, which may be the reason for the observed forming free switching behavior. Swift heavy ion irradiation is, thus, a simple but effective technique to tune the performance of HfO₂-based resistive switching devices. The study also indicates the significance of radiation damage and reliability of these devices beyond a critical fluence.

1 Introduction

Resistive random access memory (RRAM) devices have been identified as potential building blocks for future nonvolatile memory and reconfigurable hardware devices [1, 2]. RRAMs have attracted significant

attention because of their high density memory architecture [3, 4], low power consumption, faster switching [5] and longer retention time when compared to conventional nonvolatile memory (NVM) devices [6, 7]. These emerging devices are expected to replace the currently used floating gate devices, in

Address correspondence to E-mail: svnsp@uohyd.ac.in

near future [8–10]. Applications of RRAMs are not only limited to data storage devices but also to processing elements such as logic gates [11]. “In-memory computation” is envisaged with the advent of RRAM-based digital logic circuits. Based on the nature of switching mechanisms involved, RRAMs also find applications in neuromorphic systems [12, 13]. A natural consequence of the promise shown by RRAM devices is their deployment in space and nuclear electronics which operate in radiation harsh environments. It is, thus, important to study the effects of ion irradiation, radiation damage and reliability of these devices. However, such studies are very limited in literature [14–16]. Swift heavy ion (SHI) irradiation is a versatile technique to engineer material properties as well as to simulate the radiation damage in laboratory. Radiation damage produced in space over longer periods can be realized in shorter intervals by selecting appropriate species and energy. Further, the damage due to fission fragments in Nuclear reactors and radiation from solar flares/supernova can be estimated directly by SHI irradiation studies. Previous reports suggested that in general, the RRAMs are more tolerant to radiation when compared to floating gate devices [17]. However, the effects of radiation damage critically depend on the nature of materials, their phases and interfaces that constitute the device [14].

Resistive Switching (RS) behavior has been reported in many transition metal oxides including HfO_2 [4, 18, 19], ZrO_2 , Cu_xO [20], TiO_2 [21], TaO_x , WO_x [22]. HfO_2 seems to be the most promising material for future microelectronic compatible RRAMs [5, 23], in view of its success as a gate dielectric in metal oxide semiconductor (MOS) devices [24, 25]. Radiation damage studies indicate that both electron and hole traps coexist in HfO_2 , whereas only electron traps exist in SiO_2 [23, 26]. SHI irradiation can improve the performance of an HfO_2 -based MOS capacitors below a critical fluence (track overlap fluence) and the device may get deteriorated above this fluence [25]. Further, the effects of SHI irradiation critically depend on the initial phase of the material, size and shapes of the grains [27–29]. Monoclinic phase is introduced when amorphous HfO_2 is subjected to SHI irradiation. However, irradiation on an initially monoclinic phase HfO_2 resulted in the formation of tetragonal phase [29]. Previous gamma irradiation studies indicated that a low dose treatment (below 12 kGy) can improve the performance of

HfO_2 -based RRAMs. The devices are totally damaged when subjected to a dose of 48 kGy [30]. The distribution in set and reset voltages is found to increase at higher doses [19, 30]. A recent report on the effects of 1.1 GeV Au irradiation on the performance of reactive molecular beam epitaxy (RMBE) grown monoclinic- HfO_x -based RRAMs ($\text{TiN}/\text{m-HfO}_{2-x}/\text{Pt}/\text{Au}/\text{c-Al}_2\text{O}_3$) emphasizes the importance of such studies in this domain [8]. There are, however, no studies on high energy Ag ion irradiation induced performance tuning of amorphous HfO_2 -based RRAM devices.

Therefore, in this study, RF-sputtered amorphous HfO_2 has been employed as switching medium [31]. Patterned $\text{Au}/\text{HfO}_2/\text{Au}$ -based RRAM structures have been fabricated using various thin film deposition and photolithographic techniques. The effects of 120 MeV Ag irradiation on the structural properties of HfO_2 and consequent effects on the switching properties of corresponding RRAM devices have been studied. Further the effects of film thickness and the device area on the performance of RRAM devices and their radiation response have also been studied.

2 Experimental details

HfO_2 thin films, of 50 and 30 nm thickness, were produced by RF Magnetron sputter deposition from a target of 2-inch diameter and 3 mm thickness in Ar atmosphere (30SCCM). The 100 nm thickness Au top and bottom electrodes were prepared by e-beam evaporation using a 6-kW power supply for the electron gun at a constant deposition rate of 1.0 Å/s. A thin layer of 10 nm Cr was deposited by thermal evaporation on Si prior to the deposition of bottom electrode (Au) for good adhesion. The base pressure for the RF magnetron sputtering and evaporation processes were 4.2×10^{-6} and 1×10^{-6} mbar, respectively.

HfO_2 -based RRAM devices were fabricated on Si substrates (p type with 1–10 $\Omega\text{-cm}$). The standard RCA processes were employed for cleaning Si substrates [19, 32]. The devices were fabricated using standard in-house photo lithography techniques in cleanroom. A photoresist of i-line positive tone and an ultraviolet (UV) mask aligner (MJB4 of Suss Microtech) were used for photoresist exposure. Bottom electrode (BE), active layer (HfO_2) and top electrode (TE) were deposited through different masks as needed. Process flow of lithography, deposition and

lift-off has been performed at each stage. Figure 1 shows the different stages of lithography for fabricating cross bar structure of RRAM devices employed in this work.

Four sets of devices (labeled as R₁–R₄) with active area of 10 μm × 10 μm and 20 μm × 20 μm and active layer thickness of 50 nm and 30 nm were fabricated and the details are given in Table 1. Further, the SHI irradiation has been performed on R₃ and R₄ devices using the 15 MV Pelletron accelerator at the Inter University Accelerator Centre (IUAC), New Delhi to investigate the effects on the performance of these RRAM devices. For this purpose, 120 MeV Ag ion beam with a relatively low beam current of 0.5 particle-nA (pnA) was maintained throughout the experiment. The ion fluence was varied in the range of 5 × 10¹⁰ to 5 × 10¹² ions/cm², as ion beam annealing effects are expected in this fluence range [25].

The film thickness was estimated using a stylus Profilometer. Photoluminescence (PL) measurements were performed on pristine and irradiated R₃ series samples in the neighborhood of TE contact region. An excitation wavelength of 355 nm (3.5 eV which is below the bandgap of HfO₂) was employed to study defect dynamics. Current–Voltage (I–V) measurements, endurance cycles and retention tests were carried out using an Agilent technologies B1500

Table 1 The details of the RRAM devices

Device name	Device area (μm × μm)	Film thickness (nm)
R ₁	10 × 10	50
R ₂	20 × 20	50
R ₃	10 × 10	30
R ₄	20 × 20	30

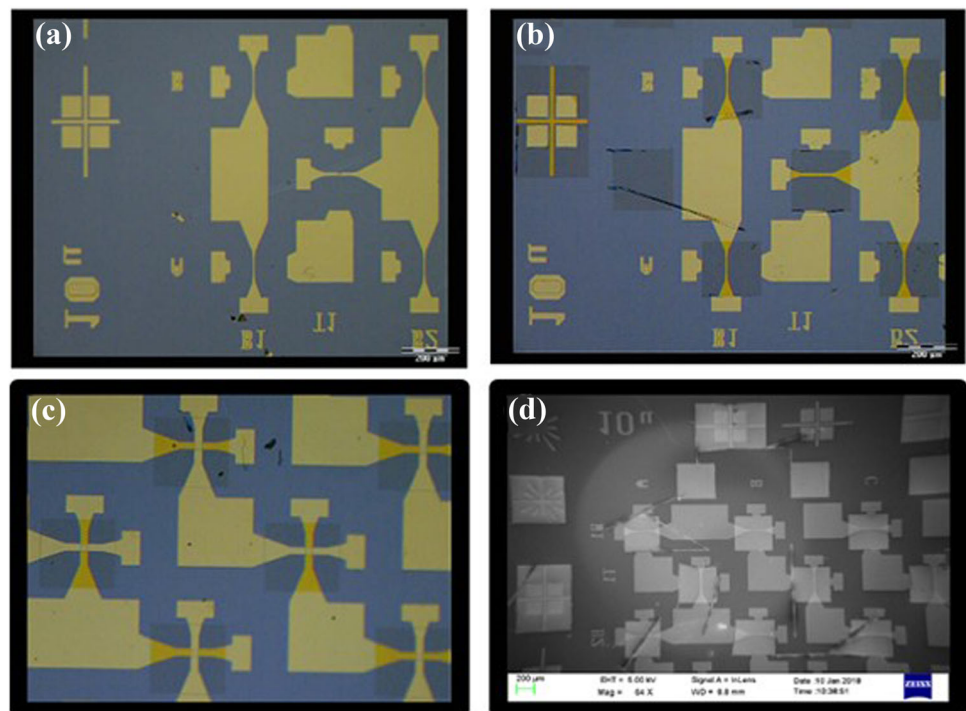
semiconductor device analyzer. Appropriate current compliance circuits are used to realize low resistance state (LRS) and high resistance state (HRS) without damaging the devices. DC sweeps of positive voltage were applied on top electrode with respect to the bottom metal (grounded) electrode. The continuous cycling pulses were applied to study the RS behavior and the endurance of these devices. The current compliance is limited to 1 mA and 18–35 mA to avoid possible hard breakdown of the device during the set and reset processes, respectively [22, 33, 34].

3 Results and discussion

3.1 Characteristics of pristine devices

I–V characteristics of devices R₁ and R₂ (representative curves) shown in Fig. 2 exhibit unipolar resistive switching behavior. Different regions in these

Fig. 1 Images showing the device structures at different processing steps, **a** step-1: bottom electrodes of width 10 μm, **b** step-2: HfO₂ film deposited on the bottom electrode through a square mask, **c** step-3: top electrode showing the cell structure and probing pads and **d** an FESEM image showing the cross bar structure of devices



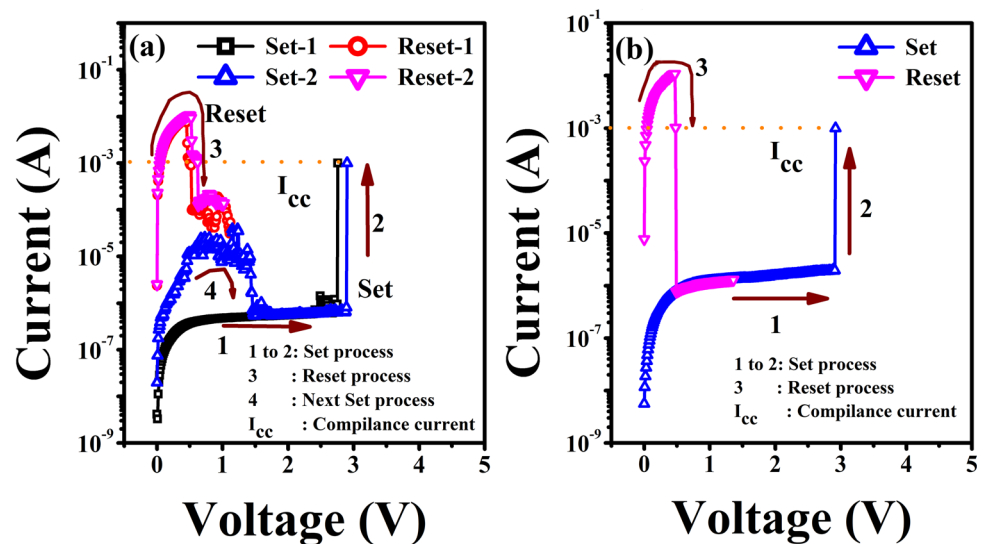
characteristics are labeled with numbers to show the paths of set (1, 2) and reset (3) operations. The forming and set voltage are found to be almost same for these devices. The set and reset voltages are found to be 2.16 V and 0.5 V respectively for the R_1 device. Similarly, set and reset voltages are 2.92 V and 0.49 V respectively for the R_2 device. A similar forming-free and unipolar RS phenomenon were earlier reported for HfO_2 -based RRAM devices [20, 35, 36] and was attributed to the formation and rupture of columnar conducting paths, known as filaments, in oxide thin film [6, 37–39]. However, bipolar switching and co-existence of bipolar and unipolar switching were also widely reported in HfO_2 -based RRAM devices [36]. It is worth noting that the electrode materials, nature of the interfaces and the phase of HfO_2 are critical in determining the switching behavior of RRAMs [8, 36, 40–44].

The present result is consistent with the previous reports, where unipolar switching was reported in HfO_2 when top electrode is Au [35, 45–48]. Forming free and unipolar switching behavior are advantageous for practical devices. It is known in literature that conductive filaments due to vacancies dominate over metal-ion-based filaments in HfO_2 [40–43]. This is particularly true when the electrodes are chemically inert, as in the present case. It is also observed that the contribution of V_o^{2+} type vacancies is significant for the formation of conducting filaments in HfO_2 when compared to that of other types of defects [40–43]. When a positive voltage is applied on the top electrode, O^{2-} ions are expected to migrate towards the top electrode, facilitating the formation of V_o^{2+}

type conducting filaments [49]. However, neither the O^{2-} nor the V_o^{2+} bind to the Au metal electrodes when voltage is removed [50, 51].

Indeed, the binding of V_o^{2+} with Au is observed to be weaker when compared to other metals [50, 51]. In addition, the possibility of out-diffusion of O^{2-} into atmosphere through the Au electrode under positive bias stress has also been reported [50–52]. The interface models that explain various types of mechanisms leading to unipolar and bipolar switching [34, 36] are not directly applicable in this study, as both the electrodes (top and bottom) are made of a chemically inert metal, Au. The combination of these two factors (out-diffusion and weak binding of V_o^{2+} to Au) and the fact that there is no interface that can act as a reservoir to store O^{2-} ions to enable the reset process when polarity is reversed causes unipolar switching. Hence, unipolar switching showed better performance when compared to the bipolar switching in these Au/ HfO_2 /Au-based RRAM devices. Therefore, the reset process can mainly be attributed to the Joule heating effects and corresponding phase changes in HfO_2 . This is consistent with the fact that higher compliance currents were required for the reset process and large dispersion observed in voltages. Several other competing processes such as the movement of vacancies in the direction of electrodes or from filaments to the resistive oxide layer or recombination with oxygen interstitials may also occur during the reset process. The reset process and the stability of the devices may further be improved by introducing an inter-layer between the top

Fig. 2 I–V Characteristics showing the RS behavior of a R_1 and b R_2 RRAM devices



electrode and the oxide with high oxygen affinity materials like Al [20] or Hf [53].

It is observed that the device R_1 did not reach complete reset (see Fig. 2a), indicating that some filaments still exist within the oxide. As a result, there is a steep increase in the current during the second set cycle (4) and an additional reset process before the actual set (5) operation. This indicates the possibility of multi-level switching in HfO_2 -based RRAM devices [18, 53, 54]. The possible out-diffusion of O^{2-} ions during the set process [50–52] may deplete the concentration of oxygen in the vicinity of top electrode. The possible gradient in oxygen concentration may further lead to the slow reset process and to introduce the observed intermediate state. This kind of gradual reset process was earlier demonstrated in RRAMs with “ $\text{HfO}_x/\text{HfO}_2$ ” bilayer as switching medium [44]. These processes can be controlled by carefully selecting appropriate interfaces, voltage windows and compliance currents as needed. The endurance cycles indicated that there is a finite spread in the set and reset voltages of these devices (R_1 – R_4). The observed non-uniform switching behavior is possible due to the randomness in the formation of filamentary conduction channels and their areal density [55, 56]. Hence the size, shape and areal distribution of filaments can significantly influence this kind of switching behavior. The spread in the set and reset voltages is found to be less for devices with smaller active area (like R_1 over R_3) as expected [57]. Here, it

is important to note that there are intermediate states in the reset cycles [18, 54], particularly for devices with smaller active area. Less number and thinner filaments are expected in devices with smaller active areas [36]. The progressive drop in the current may correspond to the reduction in the conductivity of the filaments [57, 58].

The distribution of the set voltage (V_{Set}), reset voltages (V_{Reset}) and the reset current (I_{Reset}) for all four RRAM devices have also been studied in detail. The range of I_{Reset} is found to be lesser for R_1 and R_3 when compared to that of R_2 and R_4 devices. The average I_{Reset} is estimated to be 18 mA for R_1 and 35 mA for R_2 . The number of filaments formed and their shapes depend on the active area of the device. The value of I_{Reset} depends on the previous set value which can influence the size and number density of the filaments. The number of filaments that are to be ruptured for achieving the reset is larger in the devices with larger active area [17]. Moreover, the current density is also lower in these devices, which is consistent with the literature [6]. The resistance values and cumulative distribution function (CDF) of the RRAM devices (R_1 to R_4) measured for each state are presented in Fig. 3. A positive bias voltage of 0.1 V is applied in intervals of 60 s and the current is measured to perform the retention test of these devices. These measurements were performed for each state individually (i.e., LRS or HRS) for all these devices. The resistance ratio between HRS to LRS

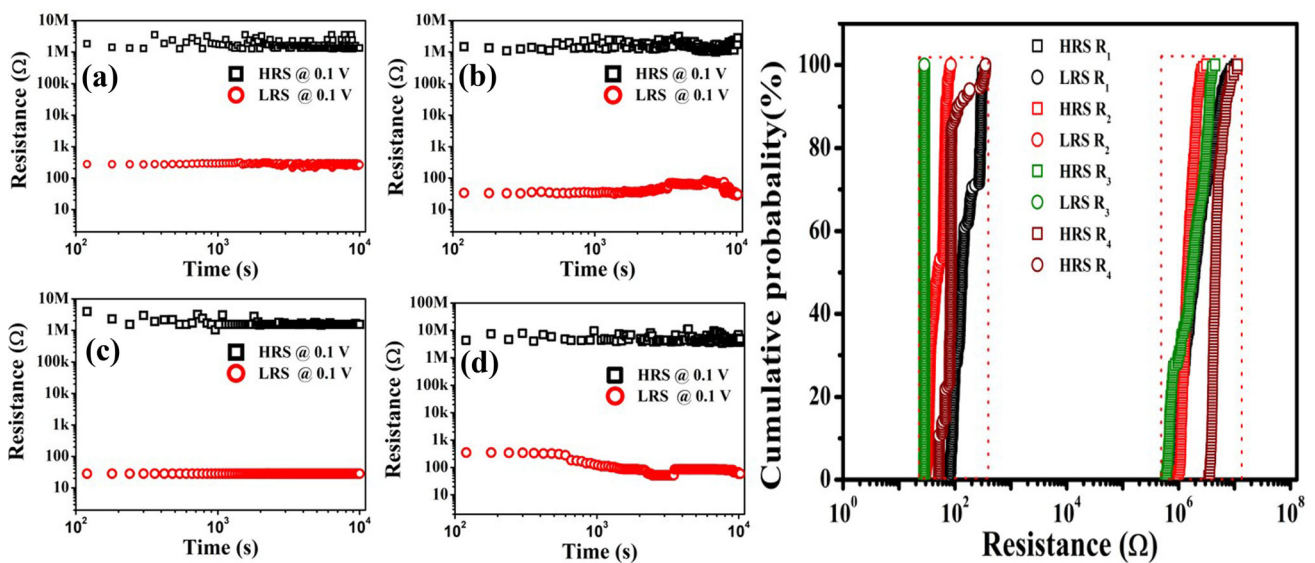


Fig. 3 The retention time (over an interval of 10^4 s) **a** R_1 , **b** R_2 , **c** R_3 , **d** R_4 of RRAM devices and **e** cumulative distribution of HRS and LRS at 0.1 V bias of R_1 to R_4 RRAM devices

($R_{\text{Off}}/R_{\text{On}}$) is estimated to be 10^4 for R_1 and R_3 and 10^5 for R_2 and R_4 devices. This demonstrates the large stability between the LRS and HRS level of these RRAM devices fabricated in this study. In fact, the state of the devices can be clearly differentiated based on their resistance (i.e., as HRS or LRS).

3.2 Effects of SHI irradiation on the performance of RRAM devices

In SHI irradiation, energetic ions interact with a material and lose their energy via electronic energy loss (S_e , which dominates for higher energies > 0.5 MeV/u) and nuclear energy loss (S_n , which dominates for lower energies < 0.5 MeV/u) [31]. The current interest in this field, is to elucidate the effects of S_e on the structural modifications of materials and consequent effects on the performance of corresponding devices. The critical value of S_e for forming ion tracks (or damaged regions) in HfO_2 is estimated to be about 20 keV/nm [29]. 120 MeV Ag ion beam is employed such that the S_e (24.86 keV/nm in HfO_2) not only dominates S_n (0.1367 keV/nm) but also remains uniform throughout the film. It is important to point out that the penetration depth of the Ag ions (range 8.49 μm) is much greater than the thickness of films. As a consequence, Ag ions will come to rest only in the substrate. The electronic energy deposition can result in deep defects and trap centers and other defects. RRAM devices (R_3 and R_4 series) were subjected to different irradiation fluences (5×10^{10} , 1×10^{11} , 5×10^{11} and 5×10^{12} ions/cm²) to study the effects on their performance. It was earlier

reported that the ion induced annealing effects dominate in this fluence range in case of HfO_2 -based MOS capacitors (MOSCAPs) [15, 25, 32]. Here, RRAM devices are subjected to similar irradiation conditions to investigate the consequent effects on their switching parameters. Figure 4 shows representative I–V curves of pristine and irradiated (R_3 series) samples indicating significant shift in the set and reset voltages as a function of fluence. The mean values of switching voltages and the corresponding distributions are shown as function of fluence in Fig. 5. Unlike MOSCAPs, RRAM exhibited an increase in the leakage current in HRS at lower fluence which may be due to the difference in initial conditions. HfO_2 films are deposited on the surfaces of Au in case of RRAMs and on the surface of SiO_2 in case MOSCAPs. Correspondingly, the average values of V_{Set} and V_{Reset} decrease with increase in fluence below the critical fluence, though the variation in V_{Reset} is not significant. Most important observation is that the ranges of V_{Set} and V_{Reset} distributions decreased up to a fluence of 5×10^{11} ions/cm² (Fig. 5). This is more evident in Fig. 6, where the endurance curves of pristine and low fluence (5×10^{11} ions/cm²) irradiations are shown. Similarly, the data of the retention test is shown in Fig. 7 for the pristine and irradiated (at critical fluence of 5×10^{11} ions/cm²) devices (of R_3). It is observed that the resistance is little lower in HRS in irradiated devices (Fig. 7b) as compared to that of the pristine devices (Figs. 7a and 3c). Similarly, the resistance is little higher in LRS. However, there is no significant change in the retention time at critical dose as

Fig. 4 I–V Characteristics showing the RS behavior of R_3 series (pristine and irradiated at different fluence) devices: **a** set curves and **b** reset curves

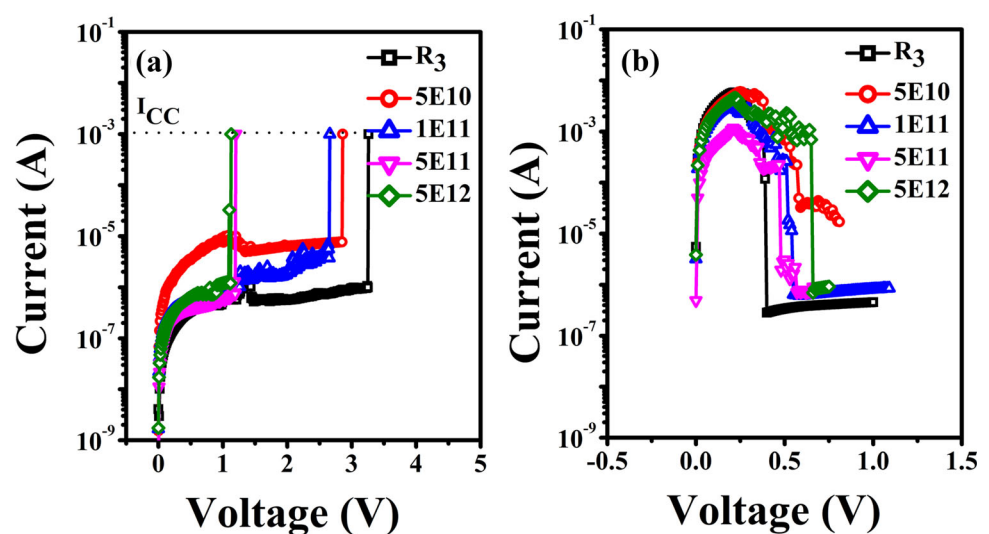


Fig. 5 The distribution of set and reset voltages of pristine and irradiated of R₃ (a, b) and R₄ (c, d) devices (Symbol represents the mean value of switching voltage and the bars represent corresponding minimum and maximum values)

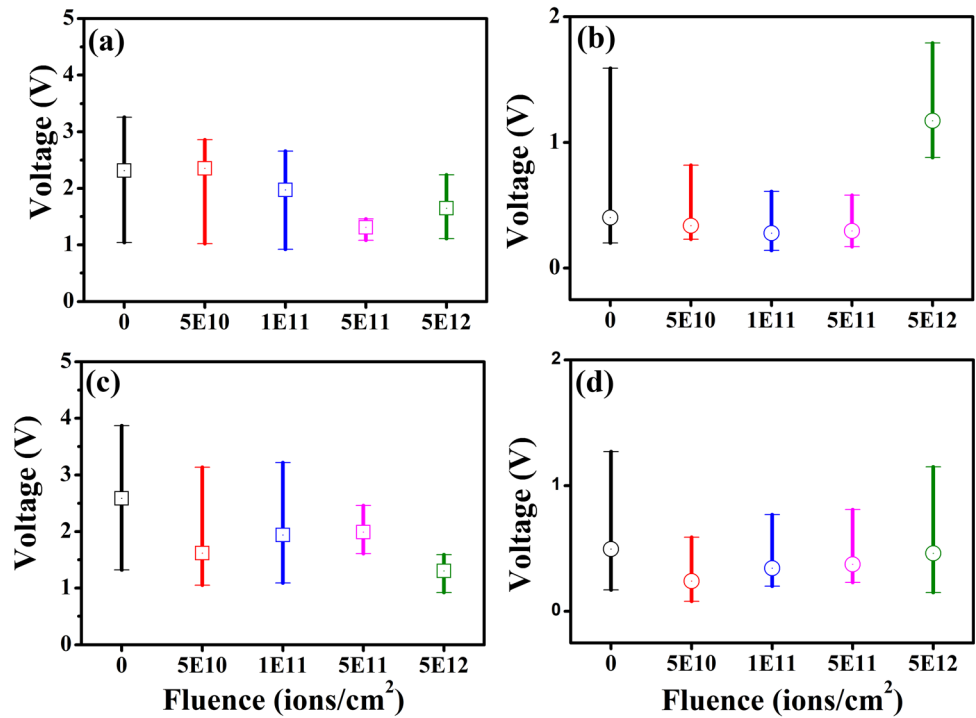
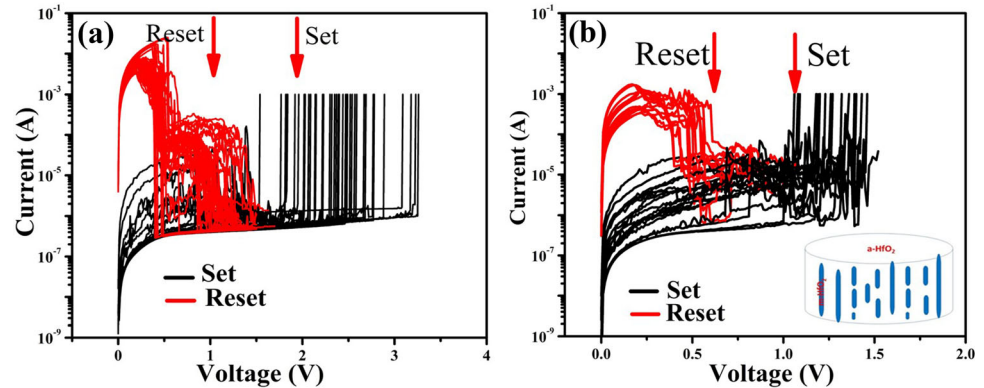


Fig. 6 Endurance curves of a pristine device and b the devices irradiated to a fluence of 5×10^{11} ions/cm²



compared to that of the pristine device. Cumulative distribution function of switching voltages and resistances ($\text{Log}(R)$) are presented in Fig. 8 for both R₃ and R₄ series devices. This analysis clearly depicts the effects of SHI irradiation on the RS behavior of RRAMs. The slopes of set/reset curves indicate a possible reduction of spread in the set and reset voltages as a function of fluence.

As stated earlier, SHI irradiation can create amorphous or crystalline tracks or columnar defects in various materials [49]. We have recently shown that the SHI irradiation can induce an amorphous to monoclinic transformation in HfO₂ nanoparticles embedded in amorphous HfO₂ thin films, above a critical fluence (5×10^{12} ions/cm²: track overlap

fluence) [29]. Hence, the formation of isolated and incomplete m-HfO₂ tracks/clusters below this fluence is also possible in the present case. The track diameters are expected to be around 10 nm [25] and the number of tracks will be of the order of fluence (i.e., $\sim 5 \times 10^{11}$ tracks / cm²). It is also important to note that the diameters of conducting filaments are also in the same range (3–10 nm) in HfO₂ [36]. It would, thus, appear that the result of the SHI process is to create a composite wherein isolated m-HfO₂ columnar tracks are embedded in the pristine a-HfO₂ matrix (as depicted as a cartoon in the inset of Fig. 6b). It is proposed that these tracks are acting as nucleation centers for filament formation under bias stress. Hence the formation of filaments in irradiated

Fig. 7 The retention time (over an interval of 10^4 s) test data of **a** R_3 —Pristine sample and **b** R_3 —Irradiated sample (critical fluence of 5×10^{11} ions/cm²)

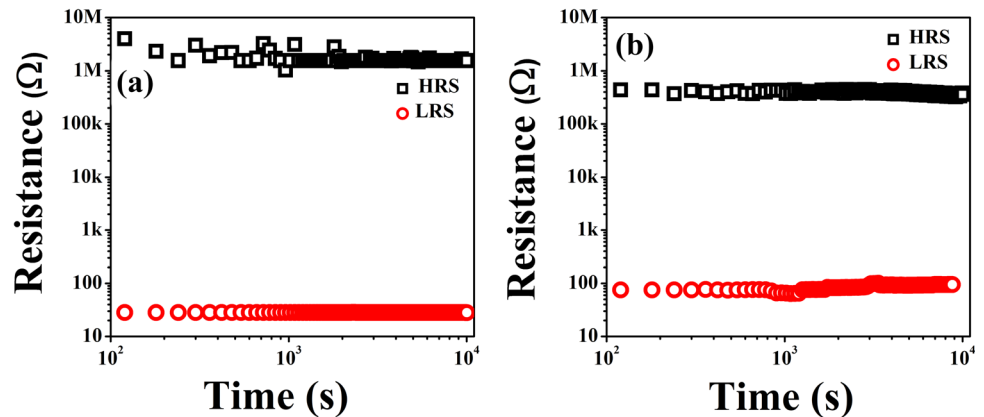
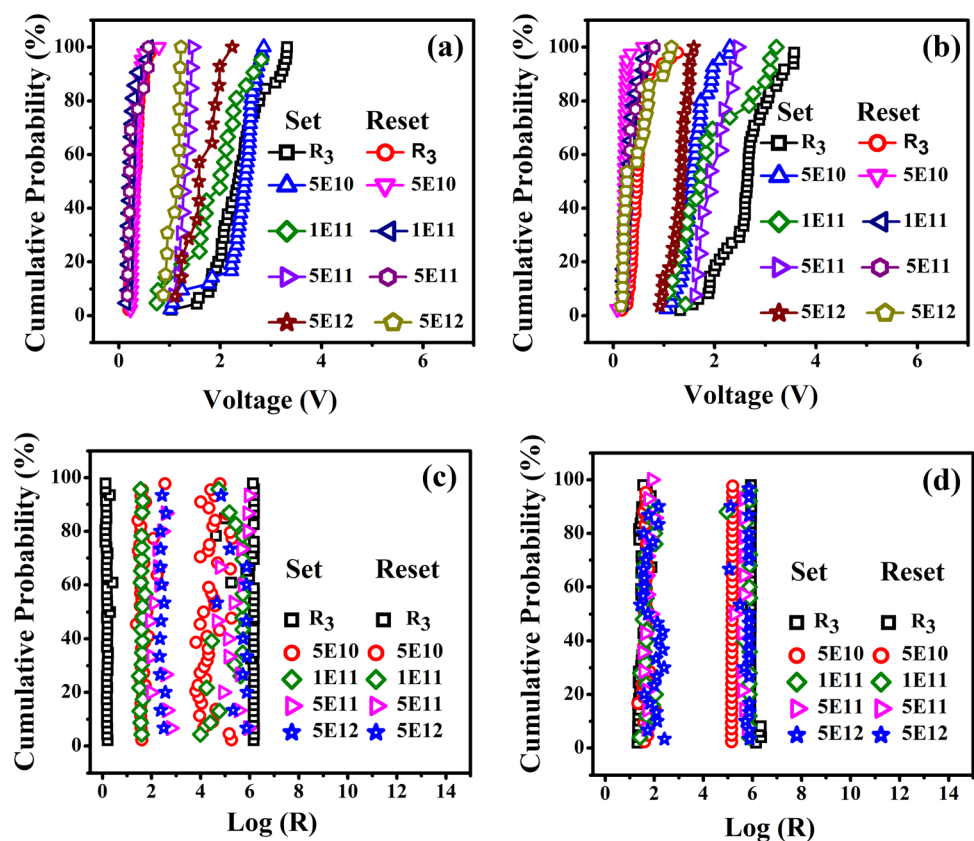


Fig. 8 The distribution of set and reset voltages of pristine and irradiated devices. Cumulative probability of set and reset voltages of **a** R_3 series and **b** R_4 series. Cumulative probability of LRS and HRS states of **c** R_3 series and **d** R_4 series



devices will not be as random as that would be in un-irradiated films. This is not only reducing the switching voltages but also reducing the spread in switching voltages. The dispersion in SET voltages is reduced significantly in devices that are subjected to low fluence (Fig. 5). The sample irradiated with a fluence of 5×10^{11} ions/cm² shows clear gap between SET and RESET voltages (See Fig. 6). Then the device gets damaged at higher doses (above track overlap fluence) leading to random switching. The overlap in the range of set and reset voltages (see

Figs. 4 and 5) beyond a critical fluence (5×10^{11} ions/cm²) is perhaps due to the production of high density of defects and/or possible ion beam mixing effects across electrode and oxide interfaces (Au/HfO₂). Nucleation centers are no longer isolated above the track overlap fluence. This is consistent with the hypothesis that the isolated tracks in irradiated samples act as nucleation centers for the formation of conducting filaments during the set process.

It is worthwhile mentioning that SHI irradiation is an efficient method to realize the isolated nucleation

centers in the switching medium. This study also suggests a scope for examining nano-wire embedded oxide layers as efficient switching media for RRAM devices. Hence the study suggests that the SHI irradiation can play a vital role in lowering the set and reset voltages and voltage ranges. Hence, a low fluence treatment of RRAM devices with SHI irradiation not only reduces the set and reset voltages but also reduces the distribution in switching voltages. However, the devices are damaged above this fluence. This is also evident from Fig. 9 which shows the number of endurance cycle vs set and reset voltages of pristine and irradiated samples.

The devices subjected to higher fluence got switched only for about 20 times out of 50 continuous set and reset cycles though the devices did not fail completely. These devices will switch again if another endurance cycle is started. However, on an average, they will switch for about 20 times out of 50 continuous cycles. This is consistent qualitatively with our earlier studies on HfO₂-based MOS devices [19, 30]. Thus, as interpreted before, beyond a critical fluence there is an overlap of ion tracks over the same device area resulting in complex damage. To identify the possible reasons for difference in behavior of pristine and SHI samples, FESEM and

photoluminescence (PL) experiments were carried out on HfO₂ films that are deposited and irradiated in same runs.

The PL measurements were performed for the R₃ sample before and after SHI irradiation. The excitation energy is chosen to be 3.5 eV, which is less than the bandgap of HfO₂. PL spectra and the deconvoluted peaks for the samples shown in Fig. 10 correspond to various types of defects in the pristine and irradiated samples [29, 59]. The fitting is performed using a peak fit program for identifying the oxygen-related vacancies in the HfO₂. Before irradiation, the peak positions are at 2.7 eV, 2.9 eV and 3.0 eV for R₃ sample. The intensity of these peaks decreases at low fluence and increases at higher fluences. The peak position at 2.7 eV can be attributed to the doubly charged positive oxygen vacancy (V_o²⁺) while the peak at 2.9 eV is associated with singly charged positive oxygen defect (V_o⁺) state [37]. The existence of these vacancy type defects in the RF sputtered a-HfO₂ films is responsible for the observed forming free switching with lower set voltages. A recent calculation [60] predicted a significant decrease in the energy barriers for creation and migration of vacancy type defects in m-HfO₂ under bias stress due to the injection of excess electrons into the oxide.

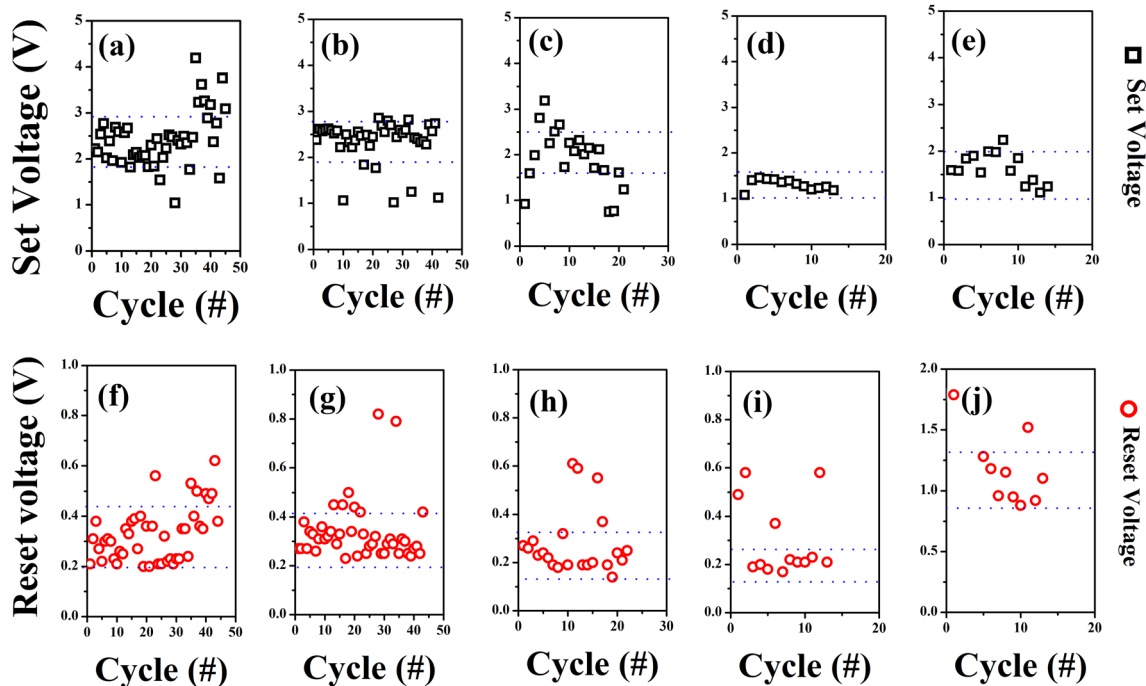
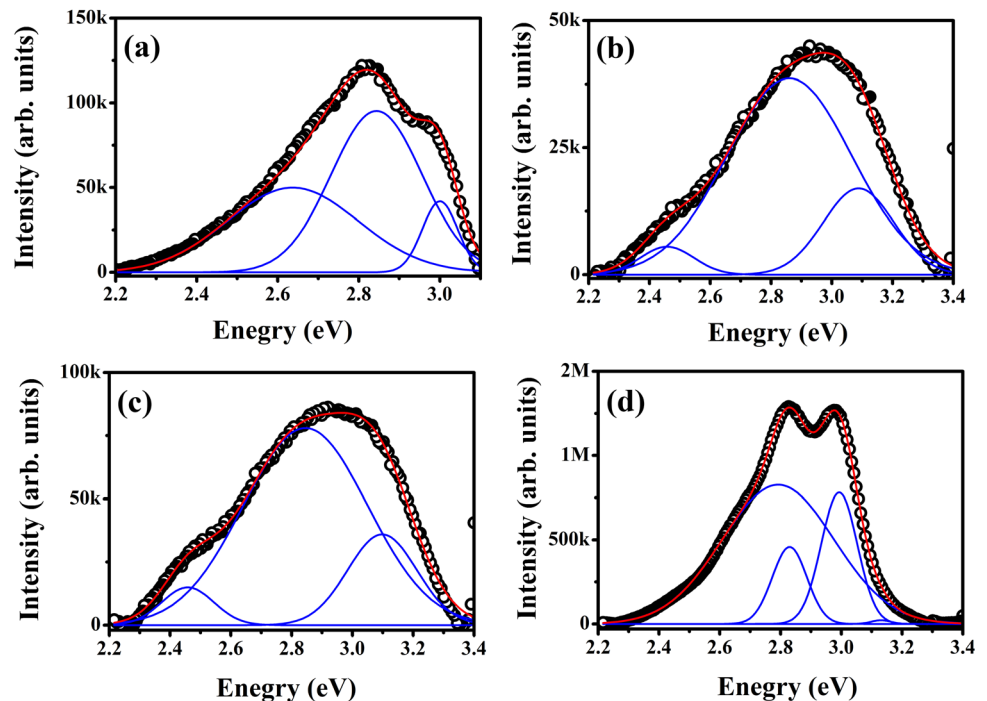


Fig. 9 The set voltage **a** R₃, **b** 5E10, **c** 1E11, **d** 5E11, **e** 5E12 ion/cm² and reset voltage **f** R₃, **g** 5E10, **h** 1E11, **i** 5E11, **j** 5E12 ion/cm², comparison over first 50 cycle of 10 μm × 10 μm RRAM devices

Fig. 10 The PL spectra of the device R₃ **a** Pristine, **b** 5E10, **c** 5E11, and **d** 5E12 ion/cm² (solid lines indicate fitting and deconvoluted peaks)



Further, we noted minor changes in the peak positions of PL spectra as a function of irradiation fluence. The changes are significant for high fluence (beyond the critical fluence). Basically, only two types of defects are populated in this case, indicating the possible re-configuration of defects as a result of SHI irradiation. The oxygen-related defects in HfO₂ films were earlier reported and most of those studies are consistent with our previous and present work [33]. In a recent study [8], it was shown that the performance of “TiN/monoclinic-HfO_{2-x}/Pt/Au” RRAMs is affected only at higher fluence (> 10¹² ions/cm²) when irradiated with 1.1 GeV Au ions ($S_e = 50.3$ keV/nm in HfO₂). Most of the devices did not experience event upset and retained the stored data even at higher fluences. However, in the present study, the active layer is an amorphous film deposited on the surface of Au by RF sputtering. The observed effects are significant even though the S_e is less (24.86 keV/nm in HfO₂) in the present study when compared to the earlier report [25]. It is, therefore, evident that SHI can be used to tune the performance parameters of such devices. Significantly, the present study also demonstrates the presence of a critical ion fluence beyond which there is deterioration in set and reset parameters, indicating the range of radiation hardness of the devices. This information is expected to be

useful for applications in nuclear and space electronics.

4 Conclusions

HfO₂-based RRAM devices were fabricated to study the effects of SHI irradiation on their performance. These devices are found to be of forming free type with unipolar switching behavior. They have exhibited good endurance cycles with high resistance ratio ($R_{Off}/R_{On} > 10^5$) and retention time. It is shown that the SHI irradiation can improve or deteriorate the performance of these devices based on the fluence. The spread in switching voltages is reduced with increase in fluence, indicating that the switching windows can be narrowed by selecting a proper combination of ion species, energy and fluence for irradiation. The set voltage is found to decrease with increase in fluence whereas the change in reset voltage is not significant. The overlap of set and reset voltages and the reduction of endurance above a critical fluence highlights the significance of radiation damage in these devices.

At lower fluences, possible creation of isolated nucleation centers, for the formation of filaments during the set process is envisaged as a reason for the observed reduction in the dispersion in set voltages.

Introduction of such isolated nucleation centers by other methods (like nano-wire embedded oxides, etc.) in switching medium can be examined in future. These RRAM devices are found to be more sensitive to the radiation damage when compared to the MOS devices. Hence, these results provide useful information to tailor as well as to study the reliability of these devices in radiation harsh environment.

Acknowledgements

N. Arun thanks UGC-NET for providing the fellowship. APP thanks National Academy of Sciences, India, Prayagraj (Allahabad) for the award of NASI Sr Scientist Platinum Jubilee Fellowship. We thank IUAC, New Delhi for financial support and for access to its facilities. We thank Centre for Nanotechnology (CFN), University of Hyderabad for providing necessary characterization facilities. We also thank DST-PURSE (India), UGC-NRC and UGC-SAP-DRS-I, CASEST, SOP, UOH programs for support.

Author contributions

All authors have significant contribution to the work and the manuscript is submitted with the consent of all authors.

Funding

UFR Project of IUAC, New Delhi, India.

Data availability

Available and can be produced anytime.

References

1. M.A. Zidan, J.P. Strachan, W.D. Lu, The future of electronics based on memristive systems. *Nat. Electron.* **1**(1), 22–29 (2018). <https://doi.org/10.1038/s41928-017-0006-8>
2. D.B. Strukov, G.S. Snider, D.R. Stewart, R.S. Williams, The missing memristor found. *Nature* **453**(7191), 80–83 (2008). <https://doi.org/10.1038/nature06932>
3. D. Ielmini, Resistive switching memories based on metal oxides: Mechanisms, reliability and scaling. *Semicond. Sci. Technol.* **31**(6), 1–25 (2016). <https://doi.org/10.1088/0268-1242/31/6/063002>
4. F. Palumbo, Formation and characterization of filamentary current paths in HfO₂-based resistive switching structures. *IEEE Electron. Dev. Lett.* **33**(7), 1057–1059 (2012). <https://doi.org/10.1109/LED.2012.2194689>
5. A. Sawa, Resistive switching in Rapid advances in information technology rely on high-speed and. *Mater. Today* **11**(6), 28–36 (2008). [https://doi.org/10.1016/S1369-7021\(08\)70119-6](https://doi.org/10.1016/S1369-7021(08)70119-6)
6. M. Lanza, A review on resistive switching in high-k dielectrics: a nanoscale point of view using conductive atomic force microscope. *Materials (Basel)* **7**(3), 2155–2182 (2014). <https://doi.org/10.3390/ma7032155>
7. A. Chen, Solid-state electronics: a review of emerging non-volatile memory (NVM) technologies and applications. *Solid State Electron.* **125**, 25–38 (2016). <https://doi.org/10.1016/j.sse.2016.07.006>
8. S. Petzold, S.U. Sharath, J. Lemke, E. Hildebrandt, C. Trautmann, L. Alff, Heavy Ion radiation effects on hafnium oxide-based resistive random access memory. *IEEE Trans. Nucl. Sci.* **66**(7), 1715–1718 (2019). <https://doi.org/10.1109/TNS.2019.2908637>
9. M. Alayan, M. Bagatin, S. Gerardin, A. Paccagnella, L. Larcher, E. Vianello, E. Nowak, B. De Salvo, L. Perniola, Experimental and simulation studies of the effects of heavy-ion irradiation on HfO₂-based RRAM cells. *IEEE Trans. Nucl. Sci.* **64**(8), 2038–2045 (2017). <https://doi.org/10.1109/TNS.2017.2721980>
10. Y. Chen, ReRAM: history, status, and future. *IEEE Trans. Electron. Dev.* **67**(4), 1420 (2020)
11. S. Kvatinisky, K. Talisveyberg, D. Fliter, A. Kolodny, U.C. Weiser, E.G. Friedman, Models of memristors for SPICE simulations, in *27th Conv. Electr. Electron. Eng. Isr.* (IEEE, 2012) pp. 1–5 (2012). <https://doi.org/10.1109/EEEI.2012.6377081>
12. X. Hong, D.J. Loy, P.A. Dananjaya, F. Tan, C. Ng, W. Lew, Oxide based RRAM materials for neuromorphic computing. *J. Mater. Sci.* **53**(12), 8720–8746 (2018). <https://doi.org/10.1007/s10853-018-2134-6>
13. R. Islam, H. Li, P. Chen, W. Wan, H. Chen, B. Gao, H. Wu, S. Yu, K. Saraswat, H. Philip Wong, Device and materials requirements for neuromorphic computing. *J. Phys. D* **52**(11), 1–24 (2019). <https://doi.org/10.1088/1361-6463/aaf784>
14. D.S. Korolev, A.N. Mikhaylov, A.I. Belov, V.A. Sergeev, I.N. Antonov, A.P. Kasatkin, O.N. Gorshkov, D.I. Tetelbaum, Influence of ion irradiation on the resistive switching parameters of SiO_x-based thin-film structures. *J. Phys. Conf. Ser.* **643**(1), 1–5 (2015). <https://doi.org/10.1088/1742-6596/643/1/012094>

15. B. Butcher, X. He, M. Huang, Y. Wang, Qi. Liu, H. Lv, M. Liu, W. Wang, Proton-based total-dose irradiation effects on Cu/HfO₂:Cu/Pt ReRAM devices. *Nanotechnology* **21**(47), 1–5 (2010). <https://doi.org/10.1088/0957-4484/21/47/475206>
16. D.M. Fleetwood, P.S. Winokur, J.R. Schwank, Using laboratory X-Ray and cobalt-60 irradiations to predict CMOS device response in strategic and space environments. *IEEE Trans. Electron. Dev.* **35**(6), 1497–1505 (1988)
17. U.S. Joshi, Ion irradiation: a tool to understand oxide RRAM mechanism. *Rad. Eff. Def. Sol.* **166**(8–9), 724–733 (2011). <https://doi.org/10.1080/10420150.2011.583246>
18. X. Lian, E. Miranda, S. Long, L. Perniola, M. Liu, J. Suñé, Threestate resistive switching in HfO₂-based RRAM. *Solid State. Electron.* **98**, 38–44 (2014). <https://doi.org/10.1016/j.sse.2014.04.016>
19. N. Arun, K.V. Kumar, A.P. Pathak, D.K. Avasthi, S.V.S. Nageswara Rao, Hafnia-based resistive switching devices for nonvolatile memory applications and effects of gamma irradiation on device performance. *Rad. Eff. Def. Sol.* **173**(3–4), 239–249 (2018). <https://doi.org/10.1080/10420150.2018.1425863>
20. L.D.V. Sangani, C.R. Kumar, M.G. Krishna, Interfacial electrode-driven enhancement of the switching parameters of a copper oxide-based resistive random-access memory device. *J. Electron. Mater.* **45**(1), 322–328 (2016). <https://doi.org/10.1007/s11664-015-4074-0>
21. L.D.V. Sangani, K.V. Sri, M.A. Mohiddon, M.G. Krishna, Low temperature Au induced crystallization of titanium dioxide thin films for resistive switching applications. *RSC Adv.* **5**(83), 67493–67499 (2015). <https://doi.org/10.1039/c5ra09022a>
22. W. Duan, J. Wang, X. Zhong, The effect of rays irradiation on the electrical properties of WO_x film-based memory cells. *Lett. J. Explor. Front. Phys.* **119**, 27003-P1-27003-P4 (2017). <https://doi.org/10.1209/0295-5075/119/27003>
23. N. Manikanthababu, N. Arun, M. Dhanunjaya, V. Saikiran, S.V.S. Nageswara Rao, A.P. Pathak, Synthesis, characterization and radiation damage studies of high-k dielectric (HfO₂) films for MOS device applications. *Rad. Eff. Def. Sol.* **170**(3), 207–217 (2015). <https://doi.org/10.1080/10420150.2014.980259>
24. N. Arun, J. Prabana, K.V. Kumar, A.P. Pathak, S.V.S. Nageswara, Fabrication of HfO₂ based MOS and RRAM devices: a study of thermal annealing effects on these devices. *AIP. Proc.* **030216**, 4–7 (2019). <https://doi.org/10.1063/1.5113055>
25. N. Manikanthababu, S. Vajandar, N. Arun, A.P. Pathak, K. Asokan, T. Osipowicz, T. Basu, S.V.S. Nageswara Rao, Electronic excitation induced defect dynamics in HfO₂ based MOS devices investigated by in-situ electrical measurements. *Appl. Phys. Lett.* **112**(131601), 1–5 (2018). <https://doi.org/10.1063/1.5012269>
26. M.R. Shaneyfelt, D.M. Fleetwood, J.R. Schwank, K.L. Hugh, Charge yield for cobalt-60 And 10-Kev X-ray irradiations Of MOS devices. *IEEE Trans. Electron. Dev.* **38**(6), 1187–1194 (1991)
27. A. Benyagoub, Mechanism of the monoclinic-to-tetragonal phase transition induced in zirconia and hafnia by swift heavy ions. *Phys. Rev. B* **72**(9), 21–24 (2005). <https://doi.org/10.1103/PhysRevB.72.094114>
28. M. Dhanunjaya, D.K. Avasthi, A.P. Pathak, S.A. Khan, S.V.S. Nageswara Rao, Grain fragmentation and phase transformations in hafnium oxide induced by swift heavy ion irradiation. *Appl. Phys. A* **124**(587), 1–10 (2018). <https://doi.org/10.1007/s00339-018-2000-z>
29. M. Dhanunjaya, S.A. Khan, A.P. Pathak, D.K. Avasthi, S.V.S. Nageswara Rao, Ion induced crystallization and grain growth of hafnium oxide nano-particles in thin-films deposited by radio frequency magnetron sputtering. *J. Phys. D* **50**, 1–8 (2017). <https://doi.org/10.1088/1361-6463/aa9723>
30. N. Arun, K. Vinod Kumar, A. Mangababu, S.V.S. Nageswara Rao, A.P. Pathak, Influence of the bottom metal electrode and gamma irradiation effects on the performance of HfO₂-based RRAM devices. *Rad. Eff. Def. Sol.* **174**(1–2), 66–75 (2019). <https://doi.org/10.1080/10420150.2019.1579213>
31. F. El Kamel, Z. Ben Cheikh, M.A. Soussou, A. Moadhen, K. Khirouni, Structural, optical and dielectric characterization of Au/HfO₂/(Pt, TiN) capacitors. *Thin Solid Films* **645**, 282–289 (2018). <https://doi.org/10.1016/j.tsf.2017.10.061>
32. N. Manikanthababu, N. Arun, M. Dhanunjaya, S.V.S. Nageswara Rao, A.P. Pathak, Gamma irradiation-induced effects on the electrical properties of HfO₂based MOS devices. *Rad. Eff. Def. Sol.* **171**(1–2), 77–86 (2016). <https://doi.org/10.1080/10420150.2015.1135152>
33. R. Waser, R. Dittmann, C. Staikov, K. Szot, Redox-based resistive switching memories nanoionic mechanisms, prospects, and challenges. *Adv. Mater.* **21**, 2632–2663 (2009). <https://doi.org/10.1002/adma.200900375>
34. P.C. Akshara, N. Basu, J. Lahiri, G. Rajaram, M.G. Krishna, Resistive switching behaviour of amorphous silicon carbide thin films fabricated by a single composite magnetron sputter deposition method. *Bull. Mater. Sci.* **43**(123), 1–8 (2020). <https://doi.org/10.1007/s12034-020-02093-8>
35. J.Y. Son, D.Y. Kim, H. Kim, W.J. Maeng, Y.S. Shin, Y.H. Shine, A HfO₂ thin film resistive switch based on conducting atomic force microscopy. *Electrochem Solid-State Lett* **14**(8), 311–313 (2011). <https://doi.org/10.1149/1.3574526>
36. H. Akinaga, H. Shima, Resistive random access memory (ReRAM) based on metal oxides. *Proc. IEEE* **98**(12),

- 2237–2251 (2010). <https://doi.org/10.1109/JPROC.2010.207083>
37. G. Sassine, L. Barbera, N. Najjari, D. Lyon, E.C. De Lyon, Interfacial versus filamentary resistive switching in TiO₂ and HfO₂ devices Interfacial versus filamentary resistive switching in TiO₂ and HfO₂ devices. *J. Vac. Sci. Technol. B* **34**(1), 012202-1-012202-6 (2016). <https://doi.org/10.1116/1.4940129>
38. K.H. Xue, B. Traore, P. Blaise, L.R. Fonseca, E. Vianello, G. Molas, B. De Salvo, G. Ghibaudo, B. Magyari-Kope, Y. Nishi, A combined ab initio and experimental study on the nature of conductive filaments in Pt/HfO₂/Pt resistive random access memory. *IEEE Trans. Electron. Dev.* **61**(5), 1394–1402 (2014). <https://doi.org/10.1109/TED.2014.2312943>
39. U. Celano, Y. Yin Chen, D.J. Wouters, G. Groeseneken, M. Jurczak, W. Vandervorst, Filament observation in metal-oxide resistive switching devices. *Appl. Phys. Lett.* **102**(12), 2011–2014 (2013). <https://doi.org/10.1063/1.4798525>
40. K.L. Lin, T.H. Hou, J. Shieh, J.H. Lin, C.T. Chou, Y.J. Lee, Electrode dependence of filament formation in HfO₂ resistive-switching memory. *J. Appl. Phys.* **109**, 084104 (2011). <https://doi.org/10.1063/1.3567915>
41. J.H. Stathis, Reliability limits for the gate insulator in CMOS technology. *IBM J. Res. Dev.* **46**(2/3), 265–286 (2002)
42. M.A. Alam, B.E. Weir, P.J. Silverman, A study of soft and hard breakdown—part II: principles of area, thickness, and voltage scaling. *IEEE Trans. Electron. Dev.* **49**(2), 232–238 (2002)
43. F. Nardi, C. Cagli, D. Ielmini, S. Spiga, Reset current reduction and set-reset instabilities in unipolar NiO RRAM, *International Memory Workshop* (2011), pp. 160–163
44. T. Tan, Du. Yihang, Ai. Cao, Y. Sun, H. Zhang, G. Zha, Resistive switching of the HfOx/HfO₂ bilayer heterostructure and its transmission characteristics as a synapse. *RSC Adv.* **8**, 41884–41891 (2018). <https://doi.org/10.1039/c8ra06230g>
45. H.Y. Lee, Y.S. Chen, P.S. Chen, T.Y. Wu, F. Chen, C.C. Wang, P.J. Tzeng, M.-J. Tsai, C. Lien, Low-power and nanosecond switching in robust hafnium oxide resistive memory with a thin Ti cap. *IEEE Trans. Electron. Dev.* **31**(1), 44–46 (2010). <https://doi.org/10.1109/LED.2009.2034670>
46. S. Lee, W.-G. Kim, S.-W. Rhee, K. Yong, Resistance switching behaviors of hafnium oxide films grown by MOCVD for nonvolatile memory applications. *J. Electrochem. Soc.* **155**(2), 92–96 (2008). <https://doi.org/10.1149/1.2814153>
47. Heng Yuan Lee, Pang Shiu Chen, Tai Yuan Wu, Ching Chiun Wang, Pei Jer Tzeng, Cha Hsin Lin, Frederick, Chen, Ming-Jinn Tsai, and Chenhsin Lien”, Electrical evidence of unstable anodic interface in Ru/HfOx/TiN unipolar resistive memory”. *Appl. Phys. Lett.* **92**, 142911 (2008). <https://doi.org/10.1063/1.2908928>
48. M.Y. Chan, T. Zhang, V. Ho, P.S. Lee, Resistive switching effects of HfO₂ high-k dielectric. *Microelectron. Eng.* **85**, 2420–2424 (2008). <https://doi.org/10.1016/j.mee.2008.09.021>
49. T. Nagata, M. Haemori, Y. Yamashita, H. Yoshikawa, Y. Iwashita, K. Kobayashi, Oxygen migration at Pt/HfO₂/Pt interface under bias operation. *Appl. Phys. Lett.* **97**, 082902-1-082902-3 (2010). <https://doi.org/10.1063/1.3483756>
50. K.M. Neyman, C. Inntam, A.V. Matveev, V.A. Nasluzov, N. Rösch, Single d-metal atoms on Fs and Fs+ defects of MgO(001): a theoretical study across the periodic table. *J. Am. Chem. Soc.* **127**, 11652–11660 (2005). <https://doi.org/10.1021/ja052437i>
51. X.-Q. Gong, A. Selloni, O. Dulub, P. Jacobson, U. Diebold, Small Au and Pt clusters at the anatase TiO₂(101) surface: behavior at terraces, steps, and surface oxygen vacancies. *J. Am. Chem. Soc.* **130**, 370–381 (2008). <https://doi.org/10.1021/ja0773148>
52. P. Gonon, M. Mougnot, C. Vallée, C. Jorel, V. Jousseume, H. Grampeix, F. El Kamel, Resistance switching in HfO₂ metal-insulator-metal devices. *J. Appl. Phys.* **107**, 074507 (2010). <https://doi.org/10.1063/1.3357283>
53. R. Nakajima, A. Azuma, H. Yoshida, T. Shimizu, T. Ito, S. Shingubara, Hf layer thickness dependence of resistive switching characteristics of Ti/Hf/HfO₂/Au resistive random access memory device. *Jpn. J. Appl. Phys.* **57**(61), 066 (2018). <https://doi.org/10.7567/JJAP.57.06HD06>
54. D.S. Jeong, H. Schroeder, U. Breuer, R. Waser, Characteristic electroforming behavior in Pt/TiO₂/Pt resistive switching cells depending on atmosphere. *J. Appl. Phys.* **104**(12), 123716 (2008). <https://doi.org/10.1063/1.3043879>
55. X. Zhang, Resistive switching characteristics of Ni/HfO₂/Pt ReRAM. *J. Semicond.* **33**(5), 2011–2013 (2012). <https://doi.org/10.1088/1674-4926/33/5/054011>
56. A. Chen, Area and thickness scaling of forming voltage of resistive switching memories. *IEEE Electron Device Lett.* **35**(1), 57–59 (2014). <https://doi.org/10.1109/LED.2013.2288262>
57. Y. Li, S. Long, Y. Liu, C. Hu, J. Teng, Q. Liu, H. Lv, J. Suñé, M. Liu, Conductance quantization in resistive random access memory. *Nanoscale Res Lett* **10**(1), 420 (2015). <https://doi.org/10.1186/s11671-015-1118-6>
58. G. Niu, P. Calka, M.A. der Maur, F. Santoni, S. Guha, M. Frasccke, P. Hamoumou, B. Gautier, E. Perez, C. Walczyk, C. Wenger, Geometric conductive filament confinement by nanotips for resistive switching of HfO₂-RRAM devices with

- high performance. *Sci. Rep.* **6**(1), 1–9 (2016). <https://doi.org/10.1038/srep25757>
59. M. Kong, B. Li, C. Guo, P. Zeng, M. Wei, W. He, The optical absorption and photoluminescence characteristics of evaporated and IAD HfO₂ thin films. *Coatings* **9**, 307 (2019). <https://doi.org/10.3390/coatings9050307>
60. J.W. Strand, J. Cottom, L. Larcher, A.L. Shluger, Effect of electric field on defect generation and migration in HfO₂. *Phys. Rev. B* **102**, 014106 (2020). <https://doi.org/10.1103/PhysRevB.102.014106>

Publisher's Note Springer Nature remains neutral with regard to jurisdictional claims in published maps and institutional affiliations.